AIMETA 2019
XXIV Conference
The Italian Association of Theoretical and Applied Mechanics
Rome, Italy, 15–19 September 2019

DEFORMABILITY ANALYSIS AND IMPROVEMENT IN STRETCHABLE ELECTRONICS SYSTEMS THROUGH FINITE ELEMENT ANALYSIS

Donato Di Vito[1], Milad Mosallaei[2], Behnam Khorramdel Vahed[2], Mikko Kanerva[1] and Matti Mäntysalo[2]

[1]Laboratory of Materials Science, Faculty of Engineering and Natural Sciences, Tampere University, 33720 Tampere, Finland
E-mails: donato.divito@tuni.fi , mikko.kanerva@tuni.fi

[2] Laboratory for Future Electronics, Faculty of Information Technology and Communication Sciences, Tampere University, 33720 Tampere, Finland E-mails: milad.mosallaei@tuni.fi , behnam.khorramdel@tuni.fi , matti.mantysalo@tuni.fi

Keywords: stretchable electronics, FEM, optimization.

Abstract. *Stretchable electronic systems employ a combination of extremely deformable substrates with electrically conductive inks printed on their surface, on which components are connected. The absence of solid metal as conductive material greatly enhances the deformability of these systems. However, although being able to sustain high deformation, the presence of rigid components heavily affects the achievable deformation levels due to strain concentrations near the interconnection area. In order to improve stretchability under these conditions, a combination of research on materials for conductive inks and optimization of the employed layout is needed. Especially for the latter, the use of Finite Element (FE) modeling is very useful, since it allows to locate critical regions for deformation behavior and to perform design optimization and instability analyses.*

In this work, the authors show the application of this strategy to improve mechano-electrical performance of the system under uniaxial tension by modelling and then modifying the overall stiffness of specific sample regions. Depending on the specific need, different strategies can be adopted to intervene on stiffness changes, such as material addition to specific regions. This work shows that, in particular, a simple technique such as laser cutting can be used to tailor the local material parameters at a deeper level, thus allowing decrease in stiffness gradients and a general enhancement of electrical performances under high levels of uniaxial deformation of the sample, as also predicted in the FE analyses.

1 INTRODUCTION

The electronics industry is currently undergoing a radical expansion of possibilities for different applications, with a particular focus on many levels of the wearables industry [3]. This event is mainly led by the recent developments in soft and stretchable electronics, which are emerging classes of electrical systems that allow completely new applications for electrical devices, such as unobtrusive sensing of specific vital signs with devices conformable to human skin. These systems differ from the standard electronics due to the high deformation that they can sustain without significant conductivity loss, which opens up a whole new range of applications for similar devices, with targets in health and biomedical applications [4], wearables [5, 6] and industrial applications [7]. These systems features a deformable substrate, on top of which conductive tracks are printed with widely different materials and fabrication processes [8, 9], with rigid components connected on top of these tracks. These elements, generally called surface mounted devices (SMDs), are typically constituted by either metallic or ceramic materials, and thus come with a higher stiffness than the elements surrounding them. This difference in stiffness consequently generates strain concentration around the SMDs when an external load is applied to the system, which in turn leads to problems related to SMD delamination or electrical failure in the conductive tracks due to crack formation. In order to avoid this phenomenon, a variety of solutions has been applied. Most of the advancements done on metallic films used as conductive tracks involve the use of different strategies to generate wavy patterns or nanoribbons in the films or the employment of serpentine layouts to design the conductive tracks in order to allow the conductive tracks increase the amount of deformation that could be applied without reaching failure by excessive deformation of the metallic layer, as mentioned more in detail in the work from Wang et al. [10] and in the work from Song et al. [11]. These strategies, although very successful for the materials employed, assume that the conductive tracks are detached from the substrate, and can freely deform in a tridimensional space. This means that the same strategies are not applicable for tracks that are bound to the substrate for different reasons. This is the case, for example, of a new class of conductive tracks constituted by a mixture of silver flakes and a binder [12, 13]. This conductive paste offers many different advantages with respect to the aforementioned metallic films, such as an the possibility to screen-print the tacks on the substrate and the possibility to print on a wide variety of materials, including textiles.
In order to improve the deformation behaviour of systems comprising conductive printed pastes, however, different strategies need to be used. One strategy, for example, is to smoothly increase the stiffness of regions that are more susceptible to strain concentration, in order to avoid deformation peaks in the vicinities of critical regions. The system's stiffness can be increased by using additional material in critical regions in order to smooth the overall deformation along the conductive tracks. This strategy was found to be effective in cases where there are interconnects, i.e. when there is a connection between a wider and a narrower line [1, 2, 14]. However, the effect of these components in systems comprising also SMDs has not yet been investigated. Also, no studies on the influence of the amount and shape of this stiffener was done. The present work focuses on that topic by investigating the effect of the angle that defines the geometrical shape of this stiffener by performing multiple FE analyses with varying stiffener shape. Thus, the angle, here called α can be defined as a parameter that, together with the base and length of the outward pointing leaves, completely defines the shape of this stiffener.

2 MATERIALS AND METHODS

In order to understand what is the effect of the stiffener's wing geometry, different models were analysed through the commercial Finite Element (FE) commercial software ABAQUS. The FE models mainly consisted of three different parts, namely the SMD, the substrate and the conductive ink. The system designed follows the dimensions required for the use of the zero-Ohm resistor SR2512, provided by TopLine. The model dimensions and main design parameters are shown in figure 1, with the thickness of the substrate and of the conductive track being,respectively, 50 and 10 μm. The characteristic element dimension for the mesh is equal to 100 μm for the substrate part and to 25 μm for the conductive track. It is important to notice that the shape of the conductive track was different for the six geometries analysed in order to investigate the effect of the interconnect design on the electromechanical properties of the system. This was achieved by keeping all the parameters constant in the analyses (as shown in figure 2) while varying the angle between the triangular stiffeners and the interconnect pads, α, which is set to vary between $140°$ and $225°$. This work focuses the results for the angles set $\{140°, 160°, 180°, 200°, 225°\}$.

The three components of the model were bound together using tie constraints since perfect

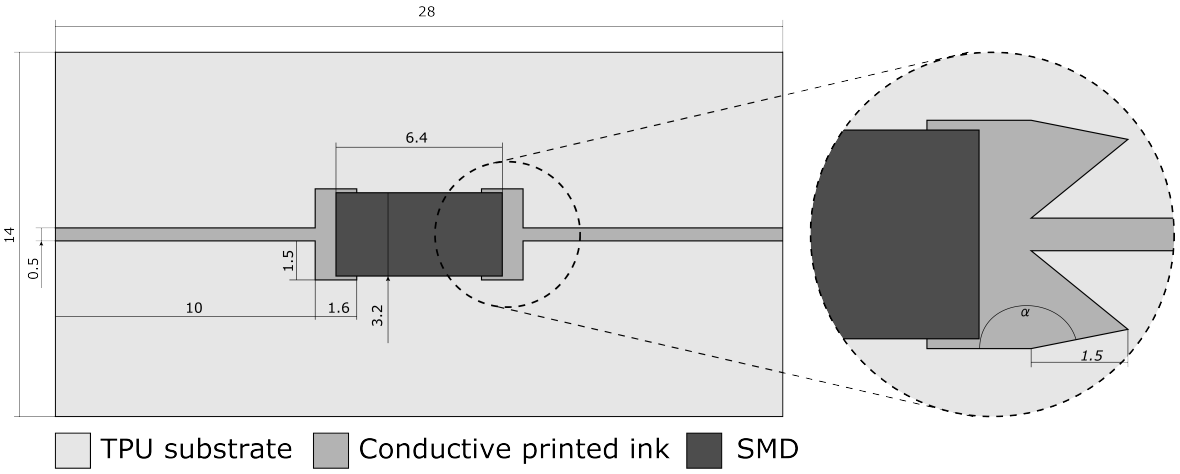

Figure 1: Dimensions of the samples analysed through the FE software. The thicknesses of the substrate and of the conductive track are respectively equal to 50 and 10 μm

adhesion was assumed between the layers. This assumption is based on previous experimental analysis: in fact, for this set of materials, electrical failure under deformation primarily occurs for conductive track cracking, and not for delamination of the conductive tracks. The models designed were subjected to tensile deformation in order to simulate a loading state that was close to the one in which electrical failure starts to occur for the system without any stiffeners. The applied displacement on the side of the specimen was thus equal to 7mm (which resulted in an overall applied deformation equal to 25%).

TPU, conductive ink and SMD were modelled by using different constitutive behaviours. In particular, TPU constitutive behaviour was assumed to behave as a Ogden incompressible hyperelastic material [15] with $N = 3$, whose strain energy density, Ψ, can be expressed as

$$\Psi = \sum_{p=1}^{3} \frac{\mu_p}{\alpha_p} \left(\lambda_1^{\alpha_p} + \lambda_2^{\alpha_p} + \lambda_3^{\alpha_p} - 3 \right) \tag{1}$$

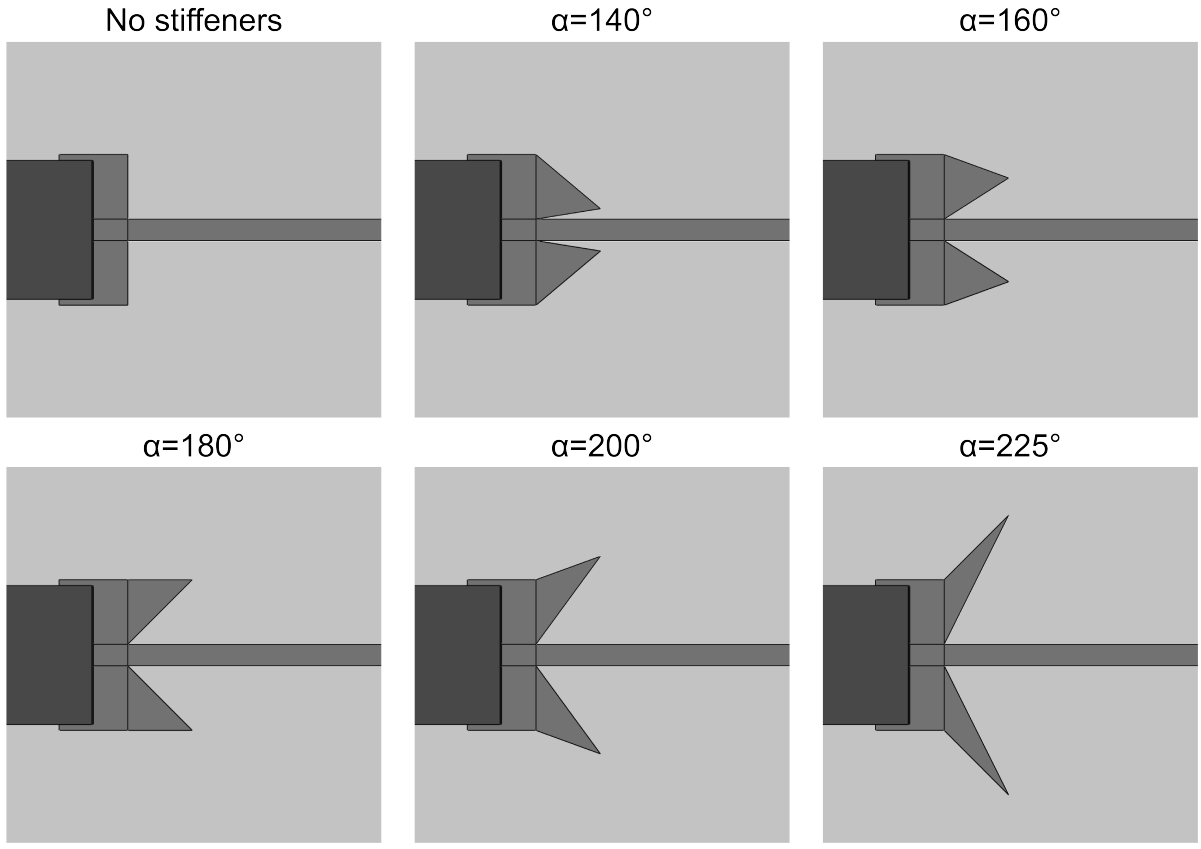

Figure 2: Shapes analysed and compared.

where $(\mu_p, \alpha_p)_{p=1,2,3}$ are material parameters and their values are reported in table 1. Due to its constituents, the conductive track is assumed to behave like a linear elastic to perfectly plastic material with isotropic hardening and two yield points. The materials parameters used are collected as well in table 1. The zero-ohm resistor, instead, was modelled as a rigid body because of the difference in stiffness between this components and the ones underlying.

3 RESULTS AND DISCUSSION

Different FE analyses were performed in order to investigate more in detail the effect of the stiffener geometry on the conductive track deformation. For these materials, in fact, resistance can be considered as a quantity that is strongly dependent from the track deformation. For metal films, in fact, the actual resistance over the resistance of the undeformed wire can be described

TPU properties			**Conductive paste properties**	
i	μ_i [MPa]	α_i	E [GPa]	1.725 GPa
1	-4.725	1.402	ν	0.3
2	1.392	3.295	Yield stress 1 [MPa]	19.67 at $\varepsilon_p = 0$
3	9.196	-2.075	Yield stress 2 [MPa]	24.35 at $\varepsilon_p = 0.0698$

Table 1: Constitutive properties used for the conductive track and TPU susbstrate material models.

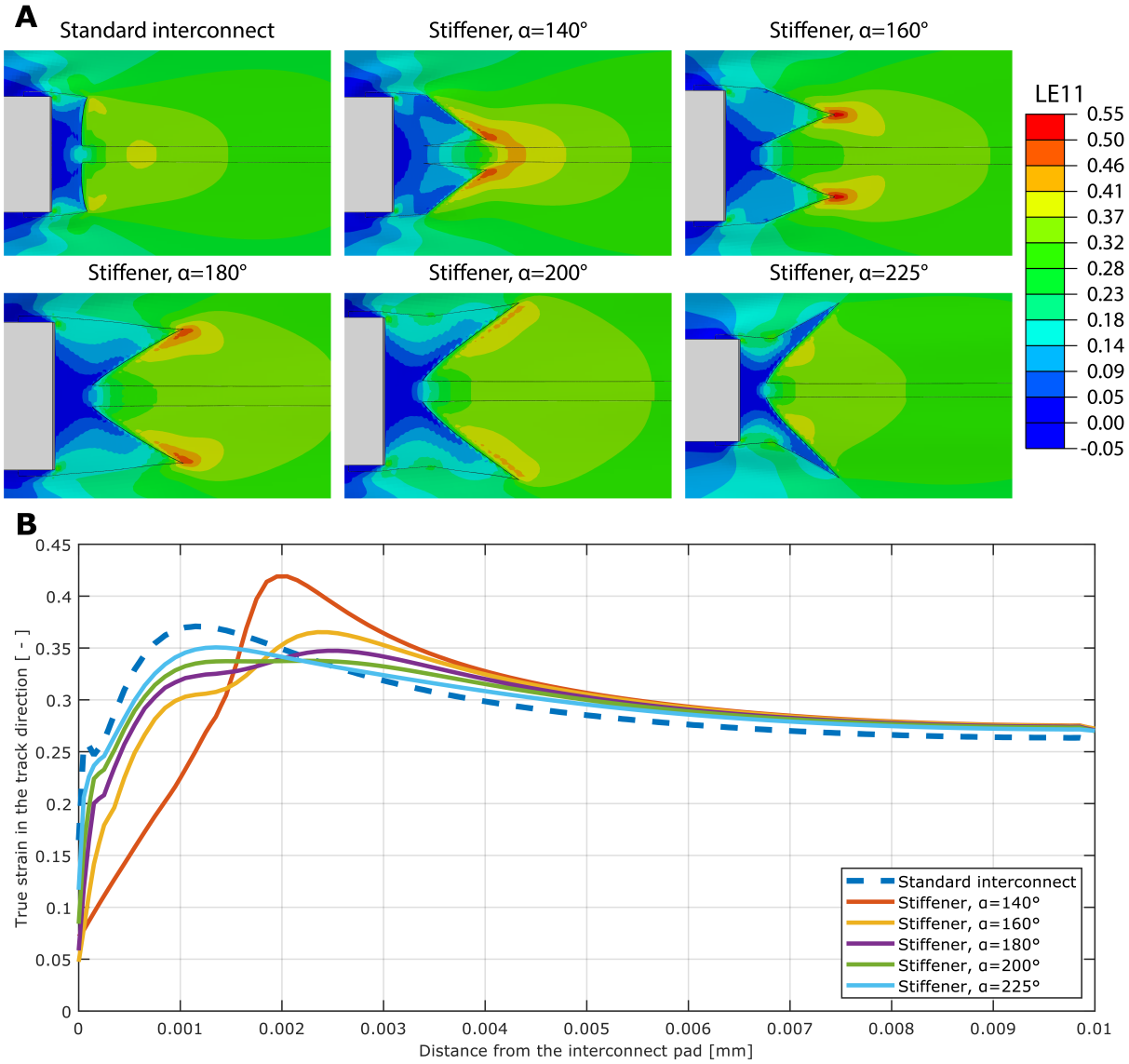

Figure 3: A) Deformation results obtained through FE analyses for the different shapes analysed. LE11 represents the local true strain in the conductive track direction, horizontal in the pictures. B) Comparison between the true strains LE11 extracted along the edges of the conductive tracks. It is possible to see that, while the results for α between $180°$ and $200°$ show a smooth change in deformation along the track, the use of a shielding structure with $\alpha = 140°$ actually shows an increase in deformation levels on the track, even with respect for the reference configuration.

by the relationship [16] $R/R_0 = (L/L_0)^2 = \lambda^2$, where L and L_0 are the actual (deformed) length and the initial one, respectively, and λ is the stretch ratio of the conductive line in the wire longitudinal direction. This relation stands for wires, thin metallic films and homogeneous conductive materials until cracking starts; however, for heterogeneous materials it is not possible to use the same relationship as great part of the loss of conductivity comes from matrix cracking and subsequent disconnection of the Ag flakes, which results in loss of conductivity. This would mean that, for this class of materials, it is extremely important to figure out the local deformation of the conductive track because that strongly interferes with its changes in resistance due to local deformation. By considering the resistivity as being constant and independent from the deformation level of the material, a better expression to describe the evolution of the

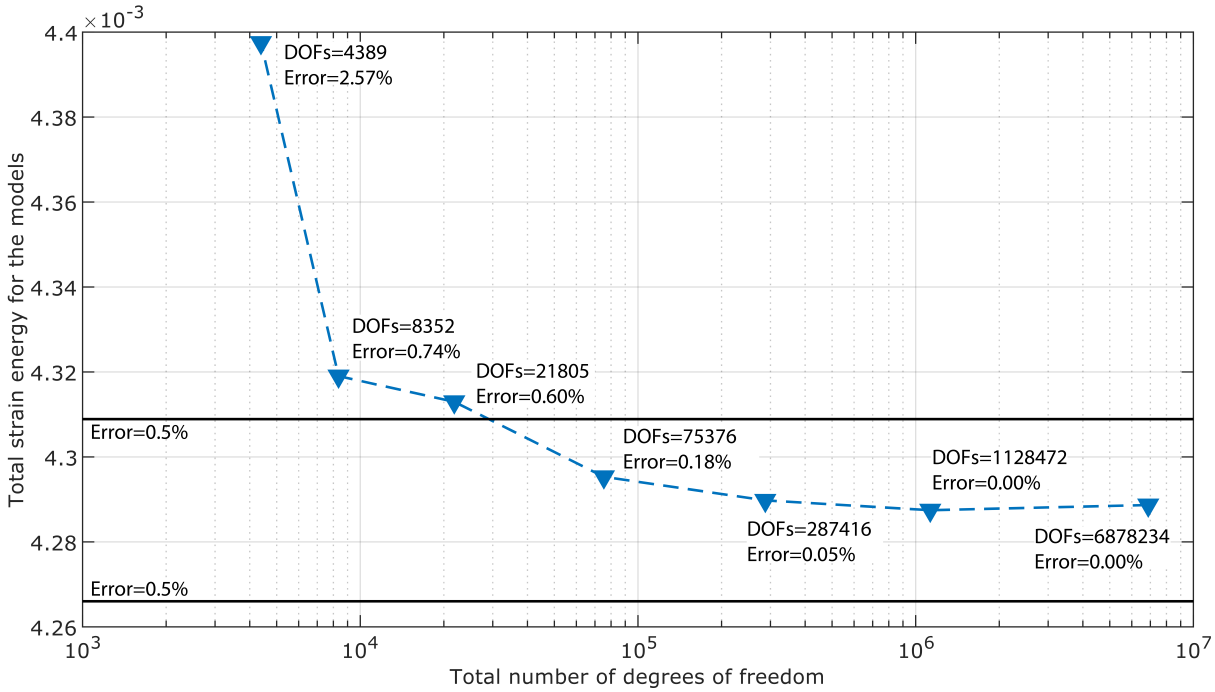

Figure 4: Strain energy convergence plot for the models analysed versus the total number of degrees of freedom. The error is estimated based on the model with the minimum energy calculated, and the black horizontal lines show the bounds for an error limit equal to 0.5%.

normalized resistance with the deformation would be:

$$\frac{R}{R_0} = \frac{L}{L_0}\frac{A_0}{A_{eff}} = \lambda\frac{A_0}{Ak(\lambda)} = \frac{\lambda^2}{k(\lambda)} \tag{2}$$

where A_{eff} is the *effective* cross-section of the conductive track, given by multiplying the deformed uncracked area A by a crack density function, $k(\lambda)$, which is equal to 1 for a conductive line with no cracks and goes to 0 for a completely disconnected conductive track. This factor is, thus, inversely dependent on the conductive track deformation, and this matter only increases the importance of finding the local deformation levels in the conductive track.
In order to ensure convergence of the solutions achieved through the FE analyses, the analysis related to the geometry with for $\alpha = 140°$ was performed with different mesh sizes, with a total number of degrees of freedom (DOFs) ranging from $\sim 4.4 \times 10^3$ (relative to a mesh size equal to 1.6mm) to $\sim 6.9 \times 10^6$ (for a mesh size equal to 25μm). The resulting strain energies from the different models are shown in figure 4 against the natural logarithm of the number of DOFs in order to show that the differences in the values of calculated reactive force at the highest amount of DOFs and at $\sim 3.0 \times 10^5$ (which is relative to the mesh sizes mentioned in section 2) is the 0.05%, clearly showing convergence for the element size used.
The deformed shapes obtained for the different FE analyses are partially represented in figure 3A, where it is possible to qualitatively appreciate that the presence of the stiffeners next to the interconnects radically changes the overall deformation field of the conductive tracks. Also the shape of the stiffeners at the interconnects greatly influence the local deformation field: in fact, while the absence of the interconnects leads to a high deformation spot at a few millimetres from the beginning of the track, the presence of stiffeners partially shields the conductive track from excessive deformation. However, when the stiffener is too close to the conductive track,

the action of the stiffener becomes detrimental for the conductivity of the track: in fact, for $\alpha = 140°$ the local deformation at a few millimeters from the interconnect becomes even higher than in the case without stiffener. Instead, for $\alpha = 200°$ and $\alpha = 225°$ the effect of the stiffness greatly decreases because of the distance from the track. For $\alpha = 160°$ and $\alpha = 180°$, the stiffeners had the biggest effect, showing that the presence of stiffer material at a certain distance from the conductive track could result in an effective shielding of the conductive track from excessive deformation. Figure 3B shows in detail the deformation values for the different designs at the edge of the track against the distance from the interconnects, which is the most critical region because it is a starting point for crack formation. This graph shows results similar to the ones seen in the upper section of the figure, as the highest level of deformation is reached with the stiffener at $\alpha = 140°$ (which, for an overall imposed deformation equal to 25% is higher than 40%), followed by the behaviour of the sample without any stiffener. It is clearer here that there are differences in the behaviour achieved with $\alpha = 160°$ and $\alpha = 180°$, since the effect of the prior lightly influences also the deformation field at the edge of the conductive track. The effect of the stiffeners with $\alpha = 180°$ and $\alpha = 200°$, instead, are very close to each other for this analysis, and thus seem preferable for applications where coexistence of deformable and rigid materials are needed.

4 CONCLUSIONS

The use of deformable materials in electronics opens the way to many interesting applications in the field of sensors for the human body and soft robotics. However, the presence of a combination of rigid and stretchable components opens up many challenges that must be tackled using a combination of the knowledge of electronics and mechanics. The presence of even more components in stretchable electronics systems further increases the level of complexity of this systems and the need to carefully design novel solution to avoid electrical failure due to static or cyclic loading, or even undesired results simply due to extreme deformations. The use of these systems together with textiles for wearable applications is one of these cases, together with ECG monitoring systems for health applications, where these systems need to offer a very high reliability and very low dependence of the behaviour from the deformation of the system. In this work, different geometries of stiffeners were analysed in order to better understand how to improve the electromechanical behaviour of systems comprising rigid and deformable components. These geometries involved the presence of additional 'edges' on the side of the conductive track in order to stiffen regions that were subjected to strain concentrations. These edges, previously called sacrificial zones, do not influence the electrical performnces of the device while, at the same time, offer a way to improve the mechanical resistance of these systems and its performances. Moreover, this additional material is applied in the printing phase together with the rest of the conductive ink, and so does not increase the number of steps in the fabrication process or increases the production time.

5 ACKNOWLEDGEMENTS

This work is funded by Business Finland (Grant no: 2947/31/2018). M. Mäntysalo is supported by Academy of Finland (grant nos. 288945, 292477). Parts of the research uses Academy of Finland Research Infrastructure Printed Intelligence Infrastructure (PII-FIRI, grant no. 320019). The authors also wish to acknowledge CSC IT Center for Science, Finland, for computational resources.

REFERENCES

[1] M. Mosallaei, J. Jokinen, M. Honkanen, P. Iso-Ketola, M. Vippola, J. Vanhala, M. Kanerva, and M. Mäntysalo, Geometry analysis in screen-printed stretchable interconnects. *IEEE Transactions on Components, Packaging and Manufacturing Technology*, **8**, 1344–1352, 2018.

[2] M. Mosallaei, J. Jokinen, M. Kanerva, and M. Mäntysalo, The effect of encapsulation geometry on the performance of stretchable interconnects. *Micromachines*, **9**, 645, 2018.

[3] T. R. Ray, J. Choi, A. J. Bandodkar, S. Krishnan, P. Gutruf, L. Tian, R. Ghaffari, and J. A. Rogers, Bio-integrated wearable systems: A comprehensive review. *Chemical Reviews*, **119**, 5461–5533, 2019.

[4] Y. Liu, H. Wang, W. Zhao, M. Zhang, H. Qin, and Y. Xie, Flexible, stretchable sensors for wearable health monitoring: Sensing mechanisms, materials, fabrication strategies and features. *Sensors*, **18**, 645, 2018.

[5] N. Matsuhisa, M. Kaltenbrunner, To. Yokota, H. Jinno, K. Kuribara, T. Sekitani, and T. Someya, Printable elastic conductors with a high conductivity for electronic textile applications. *Nature Communications*, **6**, 2015.

[6] M.A. Yokus, R. Foote, and J.S. Jur, Printed stretchable interconnects for smart garments: Design, fabrication, and characterization. *IEEE Sensors Journal*, **16**, 7967–7976, 2016.

[7] A. Koivikko, E.S. Raei, M. Mosallaei, M. Mantysalo, V. Sariola, Screen-printed curvature sensors for soft robots. *IEEE Sensors Journal*, **18**, 223–230, 2018.

[8] X. Wang and J. Liu, Recent advancements in liquid metal flexible printed electronics: Properties, technologies, and applications. *Micromachines*, **7**, 206, 2016.

[9] I.E. Stewart, M.J. Kim, and B.J. Wiley, Effect of morphology on the electrical resistivity of silver nanostructure films. *ACS Applied Materials & Interfaces*, **9**, 1870–1876, 2017.

[10] S. Wang, Y. Huang, and J.A. Rogers, Mechanical designs for inorganic stretchable circuits in soft electronics. *IEEE Transactions on Components, Packaging and Manufacturing Technology*, **5**, 1201–1218, 2015.

[11] J. Song, H. Jiang, Y. Huang, and J.A. Rogers, Mechanics of stretchable inorganic electronic materials. *Journal of Vacuum Science & Technology A: Vacuum, Surfaces, and Films*, **27**, 1107–1125, 2009.

[12] I. Locher and G. Tröster, Screen-printed textile transmission lines. *Textile Research Journal*, **77**, 837–842, 2007,

[13] K. Yang, R. Torah, Y. Wei, S. Beeby, and J. Tudor, Waterproof and durable screen printed silver conductive tracks on textiles. *Textile Research Journal*, **83**, 2023–2031, 2013.

[14] R. Moser, G. Kettlgruber, C.M. Siket, M. Drack, I.M. Graz, U. Cakmak, Z. Major, M. Kaltenbrunner, and S. Bauer, From playroom to lab: Tough stretchable electronics analyzed with a tabletop tensile tester made from toy-bricks. *Advanced Science*, **3**, 1500396, 2016.

[15] R. W. Ogden, Large deformation isotropic elasticity - on the correlation of theory and experiment for incompressible rubberlike solids. *Proceedings of the Royal Society A: Mathematical, Physical and Engineering Sciences*, **326**, 565–584, 1972.

[16] N. Lu, X. Wang, Z. Suo, and J. Vlassak, Metal films on polymer substrates stretched beyond 50%. *Applied Physics Letters*, **91**, 221909, 2007.